
Index Modulation-Aided OFDM for Visible Light Communications

Qi Wang, Tianqi Mao and Zhaocheng Wang

Additional information is available at the end of the chapter

<http://dx.doi.org/10.5772/intechopen.68885>

Abstract

Index modulation-aided orthogonal frequency-division multiplexing (IM-OFDM) is a promising modulation technique to achieve high spectral and energy efficiency. In this chapter, the conventional optical OFDM schemes are firstly reviewed, followed by the principles of IM-OFDM. The application of IM-OFDM in visible light communication (VLC) systems is introduced, and its performance is compared with conventional optical OFDM, which verifies its superiority. Finally, the challenges and opportunities of IM-OFDM are discussed for the VLC applications.

Keywords: index modulation (IM), orthogonal frequency-division multiplexing (OFDM), visible light communications (VLCs), spectral efficiency, energy efficiency

1. Introduction

Orthogonal frequency-division multiplexing (OFDM) has become a ubiquitous digital communication technique, which is widely employed in visible light communication (VLC) [1]. Since intensity modulation with direct detection is utilized in VLC for low-cost implementation, the signals modulated on the light-emitting diodes (LEDs) should be real-valued and nonnegative [2]. Therefore, various optical OFDM schemes have been proposed to satisfy these constraints, namely DC-biased optical OFDM (DCO-OFDM) [3], asymmetrically clipped optical OFDM (ACO-OFDM) [4], pulse-amplitude-modulated discrete multi-tone (PAM-DMT) [5], unipolar OFDM (U-OFDM) [6], and Flip OFDM [7]. In all these optical OFDM schemes, Hermitian symmetry is utilized on the OFDM subcarriers before inverse fast Fourier transform (IFFT), so that the time-domain signals are real-valued. To ensure the nonnegativity, DC bias can be imposed on the resultant signals, leading to low-energy efficiency. Alternatively, special arrangements on the signals in the time or frequency domain are used in Refs. [3–7] without

the need of DC bias, which generate non-negative signals at the cost of spectral efficiency loss. In order to overcome the spectral efficiency loss while maintaining high-energy efficiency, several hybrid schemes are proposed [8–11]. For example, inasymmetrically clipped DC-biased optical OFDM (ADO-OFDM) [8] and hybrid ACO-OFDM (HACO-OFDM) [9], ACO-OFDM with odd subcarriers is combined with DCO-OFDM and PAM-DMT modulating even subcarriers for simultaneous transmission, respectively. In layered ACO-OFDM (LACO-OFDM) [10] and enhanced U-OFDM (eU-OFDM) [11], multiple streams of ACO-OFDM or U-OFDM are superposed for higher spectral efficiency.

Recently, the index modulation (IM) technique has been introduced to OFDM to enhance its performance [12, 13], where the information is transmitted not only with the classic amplitude and phase modulation schemes but also implicitly by the indices of the activated subcarriers. Compared with classical OFDM, IM-aided OFDM (IM-OFDM) offers a promising trade-off between the bit error rate (BER) performance and the spectral efficiency by changing the number of activated subcarriers, the usage of constellation alphabets, and so on. In fact, the primary concept of IM-aided OFDM was proposed two decades ago, which was termed as parallel combinatory OFDM [14]. After the development of spatial modulation (SM) (or IM) in recent years, it attracts extensive attentions. In Refs. [15], subcarrier index modulation (SIM-OFDM) is proposed, where the status of each subcarrier (ON or OFF) carries one-bit information while the activated subcarriers are modulated by conventional constellations such as quadrature amplitude modulation (QAM) and phase shift keying (PSK). Additional bits can be transmitted by the indices of activated subcarriers, and the energy efficiency is improved with inactivated subcarriers. However, since the bit rate is unstable for different information bits, it may cause error propagation at the receiver. To address this issue, enhanced SIM-OFDM (ESIM-OFDM) is proposed in Refs. [16], where every two subcarriers are paired and only one subcarrier is activated in each pair. However, the spectral efficiency is reduced since the bits transmitted by indices of subcarriers are halved. In Refs. [17], OFDM with index modulation (OFDM-IM) is proposed where subcarriers are partitioned into several subblocks and the information bits are transmitted by both the indices of activated subcarriers and signal constellations in each subblock. The benefit of OFDM-IM is that less power is required since only a fraction of the subcarriers is employed for modulation, while the indices of activated subcarriers can be utilized to transmit extra bits. However, the inactivated subcarriers waste enormous precious frequency resources and reduce the spectral efficiency significantly. Moreover, it is shown that although OFDM-IM outperforms conventional OFDM with low spectral efficiency below 2 bit/s/Hz, it may perform even worse than OFDM when high-order constellations are utilized to achieve high spectral efficiency [18]. Furthermore, a subcarrier-level interleaving technique is introduced to OFDM-IM in Refs. [19], which enlarges the Euclidean distances between different transmitted symbols. In Refs. [20], OFDM-IM is combined with space-time block codes with coordinate interleaving, enhancing its BER performance due to the additional diversity gain. Besides, generalized schemes of OFDM-IM have been proposed in Refs. [21, 22], where the number of activated subcarriers of each OFDM subblock is variable, and index modulation is performed on both the in-phase and quadrature components of the modulated symbols, respectively. The generalized schemes are capable of enhancing the spectral efficiency of conventional OFDM-IM significantly. Additionally, [23] facilitates a spectrally efficient IM-OFDM scheme by employing various constellations and numbers of activated subcarriers in different subblocks. Moreover, OFDM-IM is also combined

with multiple-input-multiple-output (MIMO) systems [24, 25], yielding considerable performance improvement over conventional MIMO-OFDM. Furthermore, OFDM-IM has been applied to underwater acoustic communications as well as vehicle-to-vehicle and vehicle-to-infrastructure applications [26–28], leading to performance gains. Recently, the dual-mode index modulation-aided OFDM (DM-OFDM) is proposed in Refs. [29], where all the subcarriers are utilized to carry information unlike OFDM-IM. For each subblock, the subcarriers are divided into two groups modulated by two different constellation modes. The indices of either group can be used to transmit extra information bits. Therefore, DM-OFDM achieves higher spectral efficiency than both OFDM-IM and conventional OFDM. The generalized scheme of DM-OFDM is invoked in Refs. [30] to further enhance the spectral efficiency, where the number of subcarriers modulated by the same constellation mode is alterable. In addition, the performance trade-off of IM-OFDM schemes is investigated with theoretical analysis in Refs. [31, 32], which help to enhance the overall performance of IM-OFDM.

Due to the distinct advantages of IM-OFDM, it is also applied to VLC systems. Considering the intensity modulation property of VLC, the existent IM-OFDM schemes cannot be directly introduced to VLC, and several optical IM-OFDM (O-IM-OFDM) schemes [33, 34] have been proposed. Hence, O-IM-OFDM is investigated in this chapter by introducing the transceiver design, performing the theoretical analysis, evaluating the numerical results, and pointing out its challenges and potentials.

The rest of this chapter is organized as follows. Section 2 reviews the optical OFDM schemes for VLC, while the principles of IM-OFDM for VLC are detailed in Section 3. In Section 4, several challenges and opportunities are discussed for the deployment of IM-OFDM in VLC, and conclusions are drawn in Section 5.

2. Optical OFDM for visible light communications

Due to the intensity modulation property, the transmitted signals are constrained to be real-valued and nonnegative in VLC. Typically, Hermitian symmetry is imposed on the frequency-domain subcarriers to generate real outputs after the IFFT, and the symbols modulated onto the subcarriers satisfy

$$X_k = X_{N-k}^*, \quad k = 1, 2, \dots, N/2 - 1, \quad (1)$$

where N is the number of subcarriers in OFDM. Moreover, X_0 and $X_{N/2}$ are set to zero for the same purpose. After the IFFT, the resultant time-domain signal can be formulated as

$$x_n = \frac{1}{\sqrt{N}} \sum_{k=0}^{N-1} X_k \exp\left(j \frac{2\pi}{N} nk\right), \quad n = 0, 1, \dots, N - 1, \quad (2)$$

which is bipolar, and various techniques have been proposed to obtain nonnegative waveforms for transmission. When $N \geq 64$, the distribution of x_n is approximately Gaussian with zero mean. In the following, DCO-OFDM, ACO-OFDM, PAM-DMT, U-OFDM, and hybrid optical OFDM schemes are introduced, and the diagram of these schemes is illustrated in **Figure 1**.

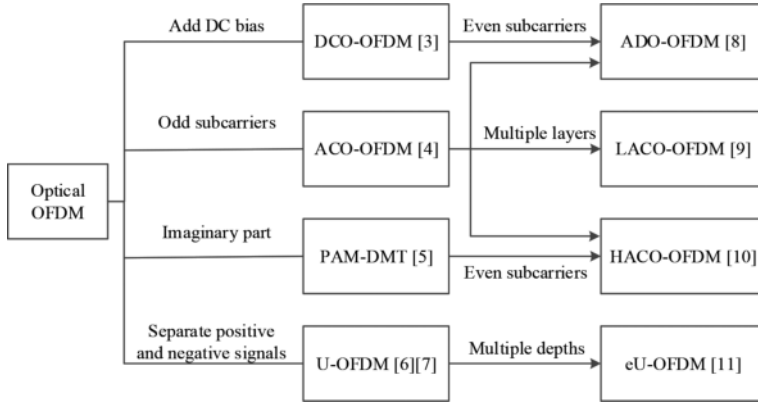


Figure 1. Diagram of optical OFDM schemes for VLC.

2.1. DCO-OFDM

A natural way to obtain the unipolar signal is adding a DC bias to the bipolar signal while clipping the remaining negative signal at zero. We denote the DC bias as x_{DC} , which is usually proportional to the square root of the electric power of x_n in Eq. (2). Since the expectation of x_n is zero, the optical power of the transmitted signal is proportional to the DC bias when clipping distortion is neglected. A large value of x_n leads to small clipping distortion, which is beneficial to the BER performance at the receiver. However, DC bias does not carry useful information, which is not energy efficient. Therefore, a trade-off between clipping distortion and energy efficiency should be made [35].

2.2. ACO-OFDM

In order to avoid DC bias to achieve higher energy efficiency, ACO-OFDM is proposed, which leaves the even subcarriers unmodulated to obtain an anti-symmetric waveform. For each positive time-domain signal, there is a negative signal with the same absolute value at certain position. Specifically, the time-domain signals of ACO-OFDM after the IFFT satisfy [4]

$$x_{ACO,n} = -x_{ACO,n+N/2}, \quad n = 0, 1, \dots, N/2 - 1, \quad (3)$$

whose negative part can be directly clipped at zero (*asymmetrically clipped*) without information loss. Therefore, the transmitted signal of ACO-OFDM is written as

$$x_{ACO,n}^c = x_{ACO,n} + i_{ACO,n} = \begin{cases} x_{ACO,n} & x_{ACO,n} \geq 0; \\ 0, & x_{ACO,n} < 0 \end{cases} \quad (4)$$

For $n = 0, 1, \dots, N - 1$, where $i_{ACO,n}$ is the negative clipping distortion of ACO-OFDM. Interestingly, the FFT of $i_{ACO,n}$ denoted as $I_{ACO,k}$ only falls on the even subcarriers, which does not interfere with the useful information. Therefore, a simple FFT can be used at the receiver for detection.

2.3. PAM-DMT

PAM-DMT is also an asymmetrically clipped method to generate nonnegative OFDM signals. Unlike ACO-OFDM, the imaginary part of all subcarriers is utilized for data transmission, while the real part is left unused to produce an anti-symmetric waveform. For the imaginary part of each subcarrier, PAM constellations are employed. The time-domain signals of PAM-DMT after the IFFT satisfy

$$x_{\text{PAM},n} = -x_{\text{PAM},N-n}, \quad n = 1, \dots, N/2 - 1, \quad (5)$$

and the transmitted signal of PAM-DMT denoted as $x_{\text{PAM},n}^c$ can be obtained similar to Eq. (4), while we denote the negative clipping distortion of PAM-DMT as $i_{\text{PAM},n}$. The FFT of $i_{\text{PAM},n}$ represented by $i_{\text{PAM},k}$ only falls on the real part of each subcarrier, which does not interfere with the useful information similar to ACO-OFDM. Therefore, a simple FFT can be employed for detection at the receiver.

2.4. U-OFDM

In U-OFDM, the signal in Eq. (2) is utilized to generate nonnegative signal. Unlike DCO-OFDM where the DC bias is used to make the signal unipolar, the OFDM frame is separated into two frames with the same length. In the first frame, all the positive signals remain the same, while the negative signals are clipped at zero. In the second frame, all the negative signals are replaced by their absolute values, while the positive signals are set to zero. At the receiver, the second frame is subtracted from the first frame to recover the original signal. Afterward, the FFT can be used to the resultant signal for detection similar to DCO-OFDM.

2.5. Hybrid optical OFDM

It is noted that, although ACO-OFDM, PAM-DMT, and U-OFDM do not require DC bias, only half of the resources (in either frequency domain or time domain) are employed compared with DCO-OFDM. Therefore, their performances are better than DCO-OFDM only when low-order constellations are used [8]. When high spectral efficiency is required, DCO-OFDM is more preferred since all the resources are used. Recently, some hybrid optical OFDM schemes have been proposed to achieve better trade-off between spectral efficiency and energy efficiency.

In ADO-OFDM, the ACO-OFDM signal is superposed by the DCO-OFDM signal, where only the even subcarriers are modulated by DCO-OFDM to avoid the interference [8]. In this way, all the subcarriers are utilized for modulation, leading to improved spectral efficiency. At the receiver, the symbols on the odd subcarriers for ACO-OFDM are firstly demodulated after the FFT. In order to detect the symbols on the even subcarriers for DCO-OFDM, the clipping distortion of ACO-OFDM should be eliminated firstly, which is estimated by the recovered symbols of ACO-OFDM. However, DC bias is still required in ADO-OFDM (although the power is reduced), which is inefficient in terms of power.

In HACO-OFDM, ACO-OFDM is combined with PAM-DMT whose even subcarriers are modulated by PAM [10]. The odd subcarriers in PAM-DMT are also left unused as in ADO-OFDM.

Therefore, it is very similar to ADO-OFDM at both the transmitter and the receiver. Since PAM-DMT does not require DC bias, HACO-OFDM is more energy-efficient compared with ADO-OFDM. However, the real part of even subcarriers is unmodulated, thus its spectral efficiency is still limited.

To fully utilize the frequency resources, LACO-OFDM is proposed in Ref. [9], where multiple layers of ACO-OFDM are combined for simultaneous transmission. Different layers employ different subcarriers to generate the nonnegative ACO-OFDM signals, while successive interference cancellation is used at the receiver to recover all the symbols in each layer. Compared with conventional ACO-OFDM, the spectral efficiency of LACO-OFDM is approximately doubled with the same constellation order. A similar method is applied to U-OFDM called eU-OFDM, which combines different depths of U-OFDM to further improve the spectral efficiency [11]. In different depths, various repetitions are required so that they can be recovered at the receiver.

3. Index modulation-aided OFDM for visible light communications

In this section, two representative IM-OFDM schemes, namely OFDM-IM and DM-OFDM, will be investigated in terms of their principles and applications in VLC.

3.1. Principles of IM-OFDM

The basic idea of OFDM-IM is to divide the subcarriers into several groups and the indices of activated subcarriers in each group can be used to convey extra information. We denote the number of subcarriers in OFDM as N , while m bits are transmitted within one OFDM symbol. The m bits are split into g groups each consisting of p bits, where we have $p = m / g$. Besides, the subcarriers are divided into g subblocks as well, and each subblock has $n = N / g$ subcarriers. In each subblock of OFDM-IM, k out of n subcarriers are activated for modulation, while the others are left empty. Therefore, the indices of the activated subcarriers can carry p_1 bits index information, which is given by

$$p_1 = \left\lfloor \log_2 \binom{n}{k} \right\rfloor, \quad (6)$$

where $\lfloor \cdot \rfloor$ denotes the integer floor operator. When M -ary constellation \mathcal{M} is used for the k -activated subcarriers, p_2 bits can be transmitted by each OFDM subblock, which is given by

$$p_2 = k \log_2(M). \quad (7)$$

Therefore, the number of total transmitted bits in an OFDM-IM frame is expressed as

$$m = g(p_1 + p_2) = g \left(\left\lfloor \log_2 \binom{n}{k} \right\rfloor + k \log_2(M) \right), \quad (8)$$

and the spectral efficiency is given by

$$\gamma_{\text{IM}} = \frac{m}{N} = \frac{\left\lfloor \log_2 \binom{n}{k} \right\rfloor + k \log_2(M)}{n} \text{ bit/s/Hz.} \quad (9)$$

Take $n = 4$, $k = 2$, $M = 2$, for example. The spectral efficiency of OFDM-IM is 1 bit/s/Hz, which is identical to the spectral efficiency of conventional OFDM scheme with BPSK modulation. Since only half of the subcarriers are activated in OFDM-IM, the energy efficiency is improved significantly.

It is shown in Eq. (6) that the number of index bits in OFDM-IM is constant when n and k are fixed. When high-order constellations are used in activated symbols, the information bits provided by the index patterns are negligible for the whole spectral efficiency. The spectral efficiency loss of the inactivated subcarriers cannot be compensated by the index bits. Moreover, frequency resource is very precious, which is unfavorable to be wasted. Therefore, DM-OFDM is proposed in Ref. [29] to fully exploit the subcarriers and index information.

In DM-OFDM, two constellation sets \mathcal{M}_A and \mathcal{M}_B are utilized for each subblock, whose sizes are M_A and M_B , respectively. In order to ensure the detection at the receiver, the two constellations sets should have no common constellations points, that is, $\mathcal{M}_A \cap \mathcal{M}_B = \emptyset$. In each subblock, the subcarriers are divided into two groups A and B , whose index sets are \mathbf{I}_A and \mathbf{I}_B . The symbols in \mathcal{M}_A and \mathcal{M}_B are used for modulation in subcarrier groups A and B , respectively. Since \mathbf{I}_B can be easily determined by \mathbf{I}_A , we denote \mathbf{I}_A as the *index pattern* of the OFDM subblock, which can be utilized to convey index bits. When k subcarriers are modulated by \mathcal{M}_A in each subblock, the number of total transmitted bits of a DM-OFDM symbol is expressed as

$$m = g \left(\left\lfloor \log_2 \binom{n}{k} \right\rfloor + k \log_2(M_A) + (n - k) \log_2(M_B) \right), \quad (10)$$

and the spectral efficiency of DM-OFDM is calculated as

$$\gamma_{\text{DM}} = \frac{m}{N} = \frac{\left\lfloor \log_2 \binom{n}{k} \right\rfloor + k \log_2(M_A) + (n - k) \log_2(M_B)}{n} \text{ bit/s/Hz.} \quad (11)$$

3.2. OFDM-IM for visible light communications

OFDM-IM can be applied to VLC with some modifications. The block diagram of OFDM-IM-based VLC system [33] is illustrated in **Figure 2**. Since intensity modulation is utilized in VLC, Hermitian symmetry is required to generate real-valued signals. Therefore, only half of the subcarriers are utilized for grouping and bit mapping, while the other half of the subcarriers can be obtained by simple Hermitian symmetry. After N -point IFFT, the bipolar signals are passed through the unipolar conversion block to generate unipolar signals for LED emission. When DC-biased optical OFDM-IM (DCO-OFDM-IM) is considered, a DC bias is utilized, while the remaining negative signals are directly clipped at zero. When unipolar OFDM-IM (U-OFDM-IM) is used, the OFDM frame is separated into two frames with the same length

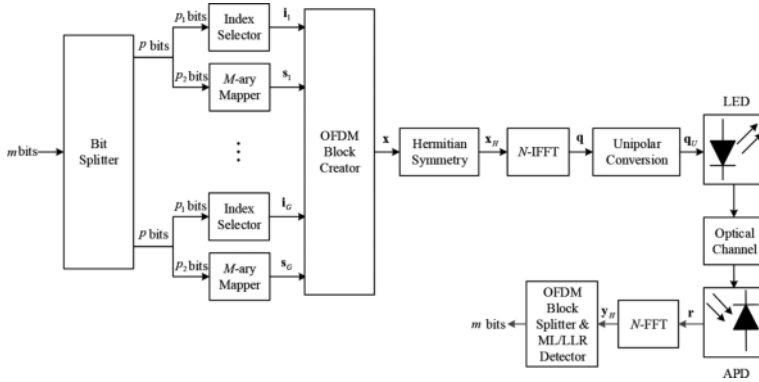


Figure 2. Block diagram of OFDM-IM-based VLC system.

similar to U-OFDM. All the positive signals are transmitted in the first frame, while the negative signals are inverted for transmission in the second frame.

Therefore, the spectral efficiencies of DCO-OFDM-IM and U-OFDM-IM are given by

$$\gamma_{\text{DCO-IM}} \approx \frac{\left\lfloor \log_2 \binom{n}{k} \right\rfloor + k \log_2(M)}{2n} \text{ bit/s/Hz}, \quad (12)$$

$$\gamma_{\text{U-IM}} = \frac{\left\lfloor \log_2 \binom{n}{k} \right\rfloor + k \log_2(M)}{4n} \text{ bit/s/Hz}. \quad (13)$$

At the receiver, if U-OFDM-IM is employed, the second frame is subtracted from the first frame. Afterward, an N -point FFT is performed on the time-domain signals. Unlike conventional optical OFDM where the detection can be performed symbol by symbol, the optical OFDM-IM requires subblock-by-subblock detection since indices of activated subcarriers are unknown at the receiver. Without loss of generality, we consider the symbols in one subblock, where the received symbols after the FFT can be written as

$$R_i = H_i X_i + W_i, \quad i = 1, 2, \dots, n, \quad (14)$$

where H_i , X_i , and W_i denote the channel response, transmitted symbol, and additive white Gaussian noise (AWGN) with the variance of N_0 in the frequency domain, respectively. When all the symbols are considered in the subblock, Eq. (14) can be rewritten in the vector form as

$$\mathbf{R} = \mathbf{H}\mathbf{X} + \mathbf{W}, \quad (15)$$

where the diagonal matrix $\mathbf{H} = \text{diag}(H_1, H_2, \dots, H_g)$. The optimal receiver employs maximum likelihood (ML) detection, which considers all the possible subblock realizations with different activated subcarrier indices and the constellation points by minimizing the metric as follows:

$$\{\hat{\mathbf{I}}, \hat{\mathbf{X}}\} = \underset{\mathbf{I}, \mathbf{X}}{\operatorname{argmin}} \|\mathbf{R} - \mathbf{H}\mathbf{X}\|^2, \quad (16)$$

where \mathbf{I} is the index pattern of the activated subcarriers. The ML detector should consider $2^{\lfloor \log_2 \binom{n}{k} \rfloor + k \log_2(M)}$ possible realizations, whose complexity is very high for large values of n , k , and M . Therefore, low-complexity detection is required for practical implementation.

In order to reduce the complexity of the receiver, log-likelihood ratio (LLR) detector is proposed by calculating the logarithm of the ratio between *a posteriori* probabilities of the frequency-domain symbols being either nonzero or zero. A larger LLR means it is more likely that the corresponding subcarrier is activated. The LLR for the i -th subcarrier is given by

$$\eta(i) = \log \left(\frac{\sum_{t=1}^M \Pr(X_i = S_t | R_i)}{\Pr(X_i = 0 | R_i)} \right), \quad 1 \leq i \leq n, \quad (17)$$

where $S_t \in \mathcal{M}$. Since $\sum_{t=1}^M \Pr(X_i = S_t) = k/n$ and $\Pr(X_t = 0) = (n - k)/n$, the LLR can be rewritten as

$$\eta(i) = \ln(k) - \ln(n - k) + \frac{|R_i|^2}{N_0} + \ln \left(\sum_{t=1}^M \exp \left(-\frac{1}{N_0} |R_i - H_i S_t|^2 \right) \right). \quad (18)$$

When the activated subcarriers are detected, the symbols on the subcarriers can be demodulated independently as the conventional optical OFDM. Therefore, the complexity of the LLR detector for optical OFDM-IM is similar to that of conventional optical OFDM.

3.3. DM-OFDM for visible light communications

The block diagram of DM-OFDM-based VLC system [34] is shown in **Figure 3**. Unlike other IM-OFDM schemes where several subcarriers are empty in each subblock, DM-OFDM utilizes two distinguishable constellation sets to modulate all the subcarriers, thus achieving higher spectral efficiency. The spectral efficiencies of DCO-DM-OFDM and U-DM-OFDM are given by

$$\gamma_{\text{DCO-DM}} \approx \frac{\lfloor \log_2 \binom{n}{k} \rfloor + k \log_2(M_A) + (n - k) \log_2(M_B)}{2n} \text{ bit/s/Hz}. \quad (19)$$

$$\gamma_{\text{U-DM}} = \frac{\lfloor \log_2 \binom{n}{k} \rfloor + k \log_2(M_A) + (n - k) \log_2(M_B)}{4n} \text{ bit/s/Hz}. \quad (20)$$

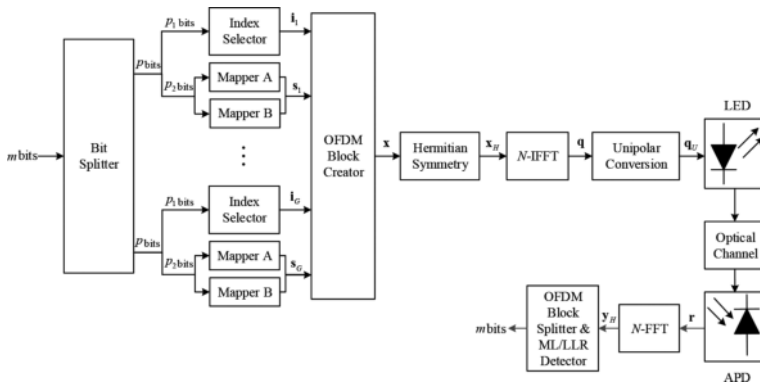


Figure 3. Block diagram of DM-OFDM for VLC systems.

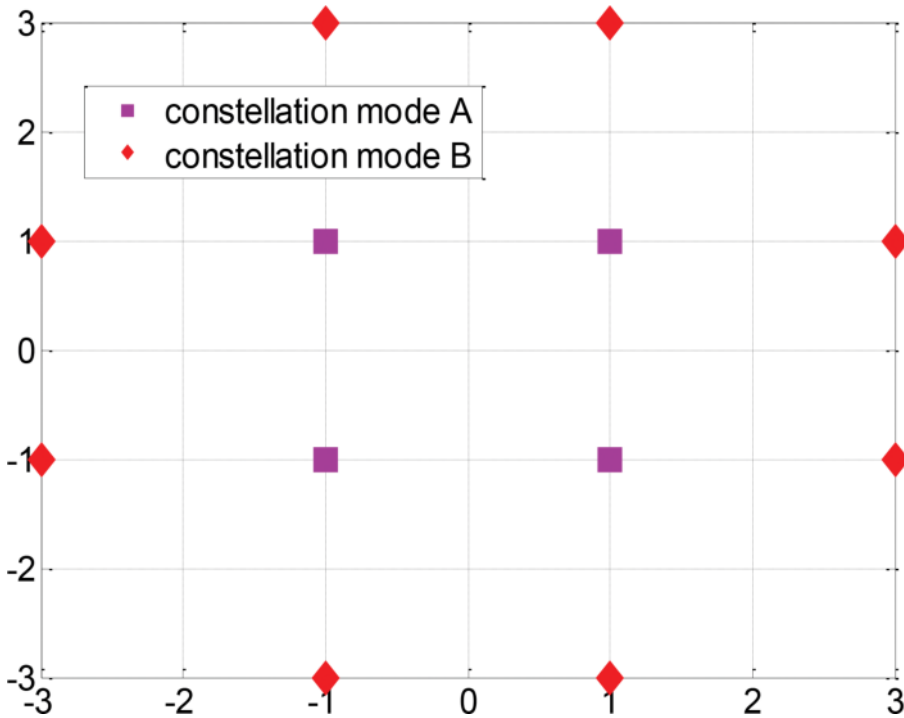


Figure 4. An example of DM-OFDM constellation design for M_A and M_B with $M_A = 8$ and $M_B = 4$.

Obviously, it is crucial to find the good combinations of two constellation sets in DM-OFDM. To ensure good BER performance, the minimum Euclidean distance between the two constellations should be equal to that of the points within each constellation. Therefore, one can firstly design a constellation with $M_A + M_B$ points and then separate the points into two constellations.

Specifically, when $M_A = M_B = M$, we can employ the points in the $2M$ -ary QAM constellation. In **Figure 4**, an example of DM-OFDM constellation design is provided for \mathcal{M}_A and \mathcal{M}_B with $M_A = 8$ and $M_B = 4$.

The detection of DM-OFDM is similar to that of OFDM-IM in a subblock-by-subblock manner. When ML detection is used, we have

$$\{\hat{\mathbf{I}}_{A'}, \hat{\mathbf{X}}\} = \underset{\mathbf{I}_{A'}, \mathbf{X}}{\operatorname{argmin}} \|\mathbf{R} - \mathbf{H}\mathbf{X}\|^2, \quad (21)$$

which still has high complexity.

The LLR detector for DM-OFDM is given by

$$\eta(i) = \ln\left(\frac{M_B k}{M_A(n-k)}\right) + \ln\left(\sum_{t=1}^{M_A} \exp\left(-\frac{1}{N_0} |R_i - H_i S_t^A|^2\right)\right) - \ln\left(\sum_{t=1}^{M_B} \exp\left(-\frac{1}{N_0} |R_i - H_i S_t^B|^2\right)\right), \quad (22)$$

where $S_t^A \in \mathcal{M}_A$ and $S_t^B \in \mathcal{M}_B$. Different from OFDM-IM, Eq. (22) calculates the logarithm of the ratio between the *a posteriori* probabilities of the frequency-domain symbols being modulated by mapper A and mapper B. When the index pattern is detected, the symbol on each subcarrier can be demodulated by the corresponding demapper.

3.4. Performance evaluation

The BER performances of OFDM-IM and DM-OFDM schemes are compared with their conventional optical OFDM counterparts in VLC systems. Unlike antennas in the radio frequency communication systems, LEDs are used in VLC systems, which have nonlinear transfer characteristics, leading to distortions on the transmitted signal beyond the linear range. The nonlinearity can be simply modeled as

$$T(x) = \begin{cases} V_{\min}, & x < V_{\min}; \\ x, & V_{\min} \leq x \leq V_{\max}; \\ V_{\max}, & x > V_{\max}; \end{cases} \quad (23)$$

where V_{\max} and V_{\min} denote the maximum and minimum allowed amplitudes, respectively.

In the simulations, the size of IFFT is set to 256, and the number of subcarriers in each subblock is 4. In OFDM-IM, 2 subcarriers are activated in each subblock. While in DM-OFDM, two subcarriers are modulated by mapper A, and the other two subcarriers are modulated by mapper B. The linear range of LEDs is $[0, 1]$, and the DC bias is set to 0.5 for DCO-OFDM, DCO-OFDM-IM, and DCO-DM-OFDM. In U-OFDM, U-OFDM-IM, and U-DM-OFDM, no DC bias is required.

Figure 5 illustrates the BER performances of OFDM-IM and the conventional optical OFDM schemes, where quadrature phase shift keying (QPSK) and binary phase shift keying (BPSK) are utilized in OFDM-IM and its conventional counterparts, respectively. In the simulations, the x -axis E_b/N_0 stands for the signal-to-noise ratio per bit. Besides, the input energies into

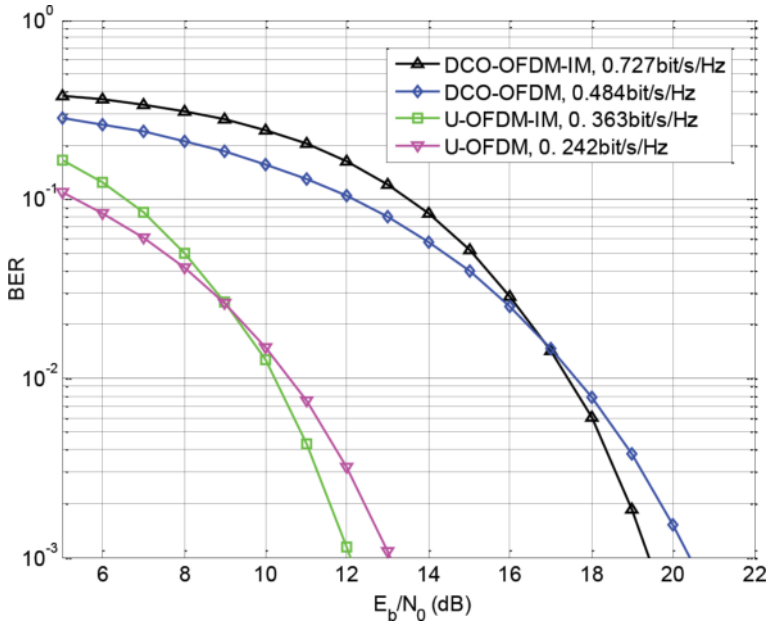


Figure 5. Performance comparison between OFDM-IM and the conventional optical OFDM schemes.

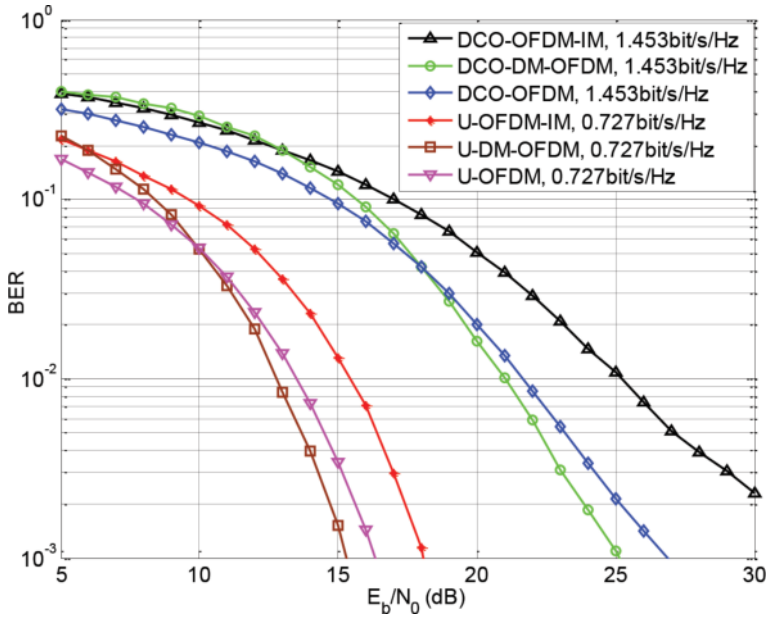


Figure 6. Performance comparison between OFDM-IM, DM-OFDM, and the conventional optical OFDM schemes at higher spectral efficiency.

LEDs are set as 13 and 13.5 dBm (not including the DC energy) for DC-based and U-based schemes, respectively. For both cases, OFDM-IM achieves about 0.243 and 0.121 bit/s/Hz spectral efficiency gains over the conventional DCO-OFDM and U-OFDM. However, it can be seen that OFDM-IM still outperforms its conventional counterparts at the BER level of 10^{-3} , since enhanced spectral efficiency leads to reduced average bit energy E_b , yielding smaller required E_b/N_0 .

When higher spectral efficiency is considered, OFDM-IM might perform even worse than conventional optical OFDM. **Figure 6** shows the BER performances of OFDM-IM, DM-OFDM and the conventional optical OFDM with a spectral efficiency of 1.453 bit/s/Hz for DC-based schemes and 0.727 bit/s/Hz for U-based schemes, where the input energies into LEDs are set as 13 and 13.5 dBm (not including the DC energy) for DC-based and U-based schemes, respectively. In conventional optical OFDM schemes, 8 QAM is employed on each subcarrier, while 32 QAM is used in OFDM-IM. In DM-OFDM, the constellations utilized are shown in **Figure 4**. From **Figure 6**, it is shown that OFDM-IM suffers from performance loss compared with conventional optical OFDM with high spectral efficiency, while DM-OFDM achieves more than 1 and 2 dB performance gains over U-OFDM and DCO-OFDM at the BER of 10^{-3} , for the reason that all the subcarriers are used for modulation, and the indices of subcarriers can provide additional dimension for transmission.

4. Challenges, opportunities, and future research trends

4.1. Dimming compatibility

In VLC systems, illumination is an important function of LEDs. Therefore, the modulation scheme should be compatible with dimming control. When the required illumination level is changed, the data rate should not fluctuate too much. In addition, the modulation scheme should support extreme illumination requirements such as very low or very high intensities. Several schemes have been proposed for conventional optical OFDM to support dimming control in VLC [36, 37], which can be extended to the IM-OFDM schemes. Furthermore, given the property of IM-OFDM, we can use different number of activated subcarriers for various illumination requirements.

4.2. MIMO transmission

In indoor environments, multiple LEDs are installed to provide sufficient illumination. Therefore, it is worthwhile to study the modulation schemes in the MIMO VLC systems [38]. For MIMO transmission, low-complexity transceiver should be designed under the intensity modulation constraint. Moreover, the index modulation can be utilized in the time domain and space domain, and multi-dimensional index modulation in time, frequency, and space domains might be useful to achieve better performance [39, 40].

4.3. Performance improvement

Current researches on IM-OFDM for VLC only consider simple combinations of optical OFDM and IM. Hybrid optical OFDM schemes introduced in Section 2.5 can be considered to further

improve the spectral efficiency of IM-OFDM for VLC systems. At the transmitter, IM-OFDM for VLC suffers from high peak-to-average power ratio (PAPR), causing nonlinear distortions of LEDs. Thus, efficient PAPR reduction techniques have to be employed to combat with the nonlinearity of LEDs. Besides, the low-complexity and high-performance receiver design also requires attention for the deployment of IM-OFDM in low-cost VLC systems.

5. Conclusions

In this chapter, to shed light on the development of IM-OFDM schemes in VLC, we introduce the principles of optical OFDM and IM-OFDM, which are exemplified by several representative schemes. It is indicated that various IM-OFDM schemes are capable of enhancing the energy efficiency or the spectral efficiency compared with conventional OFDM, leading to improved BER performance. Theoretical analysis and numerical results demonstrate that these IM-OFDM schemes can enhance the overall performance compared with its conventional counterparts. Therefore, IM-OFDM would be a promising modulation technique for future VLC systems. Moreover, the challenges and opportunities are discussed for the deployment of IM-OFDM in VLC systems, which are beneficial to researchers who are interested in this field.

Author details

Qi Wang¹, Tianqi Mao² and Zhaocheng Wang^{2*}

*Address all correspondence to: zcwang@tsinghua.edu.cn

1 School of Electronics and Computer Science, University of Southampton, United Kingdom

2 Department of Electronic Engineering, Tsinghua National Laboratory for Information Science and Technology (TNList), Tsinghua University, Beijing, China

References

- [1] Tsonev D, Chun H, Rajbhandari S, McKendry JJD, Gu E, Haji M, et al. A 3-Gb/s single-LED OFDM-based wireless VLC link using a gallium nitride μ LED. *IEEE Photonics Technology Letters*. 2014;**26**(7):637–640
- [2] Armstrong J. OFDM for optical communications. *Journal of Lightwave Technology*. 2009;**27**(3):189–204
- [3] Carruthers J and Kahn J. Multiple-subcarrier modulation for nondirected wireless infrared communication. *IEEE Journal Selected Areas in Communications*. 1996;**14**(3):538–546

- [4] Armstrong J and Lowery A. Power efficient optical OFDM. *Electronic Letters*. 2006;**42**(6):370–371
- [5] Lee S, Randel S, Breyer F, and Koonen A. PAM-DMT for intensity-modulated and direct-detection optical communications. *IEEE Photonics Technology Letters*. 2009;**21**(23):1749–1751
- [6] Tsonev D, Sinanovic S, and Haas H. Novel unipolar orthogonal frequency division multiplexing (U-OFDM) for optical wireless. In: *Proc. IEEE Veh. Tech. Conf.*; May 2012; Yohohama, Japan. pp. 1–5
- [7] Fernando N, Hong Y, and Viterbo E. Flip-OFDM for unipolar communication systems. *IEEE Transactions on Communications*. 2012;**60**(12):3726–3733
- [8] Dissanayake S and Armstrong J. Comparison of ACO-OFDM, DCO-OFDM and ADO-OFDM in IM/DD systems. *Journal of Lightwave Technology*. 2013;**31**(7):1063–1172
- [9] Wang Q, Qian C, Guo X, Wang Z, Cunningham D, and White I. Layered ACO-OFDM for intensity-modulated direct-detection optical wireless transmission. *Optics Express*. 2015;**23**(9):12382–12393
- [10] Ranjha B and Kavehrad M. Hybrid asymmetrically clipped OFDM-based IM/DD optical wireless system. *Journal of Optical Communications and Networking*. 2014;**6**(4):387–396
- [11] Tsonev D and Haas H. Avoiding spectral efficiency loss in unipolar OFDM for optical wireless communication. In: *Proc. IEEE ICC*; Jun. 2014; Sydney, Australia. pp. 3336–3341
- [12] Wen M, Cheng X, and Yang L. *Index Modulation for 5G Wireless Communications*. Springer; 2017. 154 p
- [13] Basar E. Index modulation techniques for 5G wireless networks. *IEEE Communications Magazine*. 2016;**54**(7):168–175
- [14] Frenger P and Svensson N. Parallel combinatorial OFDM signalling. *IEEE Transactions on Communications*. 1999;**47**(4):558–567
- [15] Abu-Alhiga R and Haas H. Subcarrier-index modulation OFDM. In: *Proc. 20th IEEE Int. Symp. Indoor Mobile Radio Commun.*; Sep. 2009; Tokyo, Japan. pp. 177–181
- [16] Tsonev D, Sinanovic S, and Haas H. Enhanced subcarrier index modulation (SIM) OFDM. In: *Proc. IEEE GLOBECOM Workshops*; Dec. 2011; TX, USA. pp. 728–732
- [17] Basar E, Aygolu U, Panayirci E, and Poor H. Orthogonal frequency division multiplexing with index modulation. *IEEE Transactions on Signal Processing*. 2013;**61**(22):5536–5549
- [18] Ishikawa N, Sugiura S, and Hanzo L. Subcarrier-index modulation aided OFDM-Will it work?. *IEEE Access*. 2016;**4**:2580–2593
- [19] Xiao Y, Wang S, Dan L, Lei X, Yang P, and Xiang W. OFDM with interleaved subcarrier-index modulation. *IEEE Communication Letters*. 2014;**18**(8):1447–1450

- [20] Basar E. OFDM with index modulation using coordinate interleaving. *IEEE Wireless Communications Letters*. 2015;**4**(4):381–384
- [21] Fan R, Yu Y, and Guan Y. Generalization of orthogonal frequency division multiplexing with index modulation. *IEEE Transactions on Wireless Communication*. 2015;**14**(10):5350–5359
- [22] Zheng B, Chen F, Wen M, Ji F, Yu H, and Liu Y. Low-complexity ML detector and performance analysis for OFDM with in-phase/quadrature index modulation. *IEEE Communication Letters*. 2015;**19**(11):1893–1896
- [23] Yang X, Zhang Z, Fu P, and Zhang J. Spectrum-efficient index modulation with improved constellation mapping. In: *Proc. IEEE HMWC*; Oct. 2015; Xi'an, China. pp. 91–95
- [24] Basar E. Multiple-input multiple-output OFDM with index modulation. *IEEE Signal Processing Letters*. 2015;**22**(12):2259–2263
- [25] Basar E. On multiple-input multiple-output OFDM with index modulation for next generation wireless networks. *IEEE Transactions on Signal Processing*. 2016;**64**(15):3868–3878
- [26] Wen M, Cheng X, Yang L, Li Y, Cheng X, and Ji F. Index modulated OFDM for underwater acoustic communications. *IEEE Communications Magazine*. 2016;**54**(5):132–137
- [27] Wen M, Li Y, Cheng X, and Yang L. Index modulated OFDM with ICI self-cancellation in underwater acoustic communications. In: *Proc. IEEE Asilomar Conf. Signals, Syst, Comput.*; Nov. 2014; Pacific Grove, CA, USA. pp. 338–342
- [28] Cheng X, Wen M, Yang L, and Li Y. Index modulated OFDM with interleaved grouping for V2X communications. In: *Proc. IEEE Int. Conf. Intell. Transp. Syst.*; Oct. 2014; Qingdao, China. pp. 1097–1104
- [29] Mao T, Wang Z, Wang Q, Chen S, Hanzo L. Dual-mode index modulation aided OFDM. *IEEE Access*. 2017;**5**:50–60
- [30] , Mao T, Wang Q, and Wang Z. Generalized dual-mode index modulation aided OFDM. *IEEE Communication Letters*. 2017;**21**(4):761–764
- [31] Wen M, Cheng X, and Yang L. Optimizing the energy efficiency of OFDM with index modulation. In: *Proc. IEEE Int. Conf. Commun. Syst.*; Nov. 2014; Macau, China. pp. 31–35
- [32] Li W, Zhao H, Zhang C, Zhao L, and Wang R. Generalized selecting sub-carrier modulation scheme in OFDM system. In: *Proc. IEEE ICC Workshops*; Jun. 2014; Sydney, NSW, Australia. pp. 907–911
- [33] Basar E, Panayirci E. Optical OFDM with index modulation for visible light communications. In: *Proc. IEEE Int. Workshops on Opt. Wirel. Commun.*; Sep. 2015; Istanbul, Turkey. pp. 11–15
- [34] Mao T, Jiang R, and Bai R. Optical dual-mode index modulation aided OFDM for visible light communications. *Optics Communications*. 2017;**391**:37–41

- [35] Wang Z, Wang Q, Chen S, and Hanzo L. An adaptive scaling and biasing scheme for OFDM-based visible light communication systems. *Optics Express*. 2014;**22**(10):12707–12715
- [36] Wang Q, Wang Z, and Dai L. Asymmetrical hybrid optical OFDM for visible light communications with dimming control. *IEEE Photonics Technology Letters*. 2015;**27**(9):974–977
- [37] Wang Q, Wang Z, Dai L, and Quan J. Dimmable visible light communications based on multilayer ACO-OFDM. *IEEE Photonics Journal*. 2016;**8**(3)
- [38] Wang Q, Wang Z, and Dai L. Multiuser MIMO-OFDM for visible light communications. *IEEE Photonics Journal*. 2015;**7**(6)
- [39] Basar E, Panayirci E, Uysal M, and Haas H. Generalized LED index modulation optical OFDM for MIMO visible light communications. In: *IEEE ICC 2016; May 2016; Kuala Lumpur, Malaysia*
- [40] Sugiura S, Chen S, and Hanzo L. Generalized space-time shift keying designed for flexible diversity-, multiplexing- and complexity-tradeoffs. *IEEE Transactions on Wireless Communications*. 2011;**10**(4):1144–1153

